SOME HIGH-SPEED FLUTTER STUDIES

By I. E. Garrick

Langley Memorial Aeronautical Laboratory

It is intended to present a brief review and progress report of some of our recent studies on flutter at high speeds. In order to present this work with a degree of continuity, it is perhaps desirable to make a few observations of general interest on the past stream of flutter work.

The field of flutter is concerned essentially with a study of the circumstances whereby a complicated elastic structure such as an aircraft or aircraft component can spontaneously become a "flutter" machine and absorb energy from the airstream to the extent of damaging or destroying itself. Hence it would appear that knowledge of nonstationary aerodynamic phenomena is a basic requirement to our understanding of flutter. Yet in the old days (some twenty years ago) flutter was discussed without this knowledge of even the low-speed air forces, and analysis employed either statically determined aerodynamic coefficients or, as continues even to the present day, a set or matrix of numbers arrived at by some combination of reason, guess, and hope.

Although these older investigations sometimes led to some misleading specific rules, nevertheless they also led to certain basic principles for flutter prevention. Thus, the basic safeguards of (a) increased stiffness, (b) avoidence of coupling (implying, for example) proper mass balance, and (c) sufficient damping - followed without specific knowledge of the air forces.

The detailed questions of what kind of stiffness, how much stiffness, how to attain it; how much mass balance, where to put it, what modes to balance against; how much damping is needed, how reliable is the damping available, how "irreversible" is irreversible when applied to control surfaces such as tabs. These and similar questions are not yet answered in general but only in special circumstances, for these questions are tied up with elastic problems which are too complex to be anything but approximately handled, even without consideration of air forces, and with aerodynamic problems which are complicated enough even in the steady case and for rigid structures.

Yet the accumulated experience in flutter is of formidable quantity (as anyone who has struggled with the flutter field can attest) and represents information obtained by combinations of statistical studies, analysis, theory, and testing.

An example of a distillate of this experience in the form of recommended procedures in design is the Army, Navy, Commerce bulletin, soon to be made available: ANC-12 (1) "Procedure for Aircraft Structural Vibration Survey" and ANC-12 (2) "Methods of Flutter Prevention" Another example is the torsional stiffness criterion of reference 1.

Although stiffness criteria and similar procedural rules of thumb can be of great practical help they should not serve as a substitute for thought or camouflage the need for understanding.

Before discussing the experimental studies I would like to give a thumb-nail sketch of the theoretical basis for study of the aerodynamic forces and some of the implications. I intend to present only the governing field equations and their significance without going into any mathematical details.

The general nonstationary flow equations for irrotational potential flow of a compressible fluid can be expressed in an invariant form:

$$\frac{1}{c^2}\left(\frac{\partial}{\partial t} + \bar{v}\cdot\nabla\right)^2 \phi = \nabla^2\phi \qquad (1)$$

where the differential symbols $\frac{\partial}{\partial t}$ and $\bar{v}\cdot\nabla$ $\left(= v_x \frac{\partial}{\partial x} + v_y \frac{\partial}{\partial y} + v_z \frac{\partial}{\partial z}\right)$ operate only on the velocity potential ϕ (not on v) and where, for the adiabatic pressure-density relation, the local (variable) speed of sound is

$$c^2 = c_o^2 - \frac{\gamma - 1}{2} v^2$$

The compressible-flow equations have not, so far as I am aware, been given this wave-equation form before and perhaps that is a valid reason for showing it here. The potential is propagated in the manner of a wave disturbance of finite amplitude throughout a medium in which the velocity of sound is variable.

The invariant form serves to unify the general compressible potential-flow picture, at least for purposes of discussion. For example when $\frac{\partial}{\partial t}$ is absent and the disturbance not necessarily small the equation becomes the one treated by Raleigh, Janzen, and

Poggi. In a space of one dimension, for example, it reduces to the equation of Riemann for aerial plane waves of finite amplitudes. (For $c = \infty$, it reduces to the incompressible case.)

For small disturbances from a main stream V in the x-direction the original nonlinear equation becomes a linear one and c is now treated as a constant

$$\frac{1}{c^2}\left(\frac{\partial}{\partial t} + V\frac{\partial}{\partial x}\right)^2 \phi = \nabla^2\phi \qquad (2)$$

This equation contains the equation for the propagation of sound ($V = 0$), the equation leading to thin-airfoil theory and the Prandtl-Glauert and Ackeret rules in steady flow, and the equation treated by Possio and others for subsonic and supersonic non-stationary flow. The treatment of flow in a plane on the basis of this equation is in pretty fair shape and a number of theoretical papers and applications exist but much remains to be done on the handling of finite-span problems. (See references 2 and 3.)

In the near sonic region the linearized theoretical basis clearly requires modification as indicated by the Prandtl-Glauert and Ackeret rules leading to infinite slopes of the lift curve at $M = 1$. It is likely that in this region it is necessary to employ iterative methods and to take into account second-order and other effects (including viscosity and shape factors) but even the small-disturbance equation appears differently. Thus, if all velocities are only slightly different from the velocity of sound c^*, and the main stream is in the x-direction, there is obtained for the equation satisfied by the velocity potential

$$\frac{1}{c^{*2}}\left(\frac{\partial}{\partial t} + c^*\frac{\partial}{\partial x}\right)^2 \phi = \nabla^2\phi + (\gamma + 1)\,\phi_{xx}\left(1 - \frac{\phi_x}{c^*}\right) \qquad (3)$$

or

$$(\gamma + 1)\,\phi_{xx}\left(1 - \frac{\phi_x}{c^*}\right) + \phi_{yy} + \phi_{zz} - \frac{1}{c^{*2}}\left(\phi_{tt} + 2c^*\phi_{xt}\right) = 0$$

This equation reduces in the steady case to a nonlinear equation leading to the transonic similarily rules discussed by von Karman in his Wright lecture. With this small background of theoretical considerations it is apparent that the detailed flow

picture in the nonstationary case, particularly at near sonic speeds, can become very complicated. But in this subject we often have to postpone our understanding of details in order to obtain knowledge, in reasonable time, of integrated effects. Information on some of these integrated effects was the objective of the first phase of our experimental work.

Study of torsion-bending wing flutter at high speeds has been made by means of wind-tunnel testing and also with the aid of recently pioneered techniques employing bomb drops and rockets.

The scope of the wind-tunnel investigation which was made in the Langley 4.5-foot flutter-research tunnel, is indicated in figure 1. The models were cantilever wings which were simply built since flutter fatalities were many. They were mainly of wood construction, many with suitable metal inserts, a few had ribs and spars covered with fabric. A range of semispan-chord ratios is covered, a range of sweep including some types of built-in sweep and rotated models and some tapered wings.

Figure 2 shows a particular swept wing mounted as a cantilever in the Langley 4.5-foot flutter-research tunnel. Two noteworthy features of this wind tunnel are the 30 to 1 possible density change in the medium and the relatively high Mach numbers attained at different density conditions with low power by the use of mixtures of air and Freon-12. Some erratic results have been obtained near top tunnel speeds corresponding to choking conditions but in general the tunnel data taken at Mach numbers below 0.8 are considered reliable.

Figure 3 shows a high-speed-rocket flutter vehicle. It has a top speed corresponding to about $M = 1.5$, an acceleration of about 50 g. Its weight is about 100 pounds. It is the high acceleration type of rocket which experienced a large number of failures when originally used for aerodynamic tests and which led to the empirical torsional-stiffness criterion given in reference 1.

This test vehicle is at present used for exploratory flutter testing and employs a break-wire to determine time of wing failure (reference 4). Telemeter equipment for it is also being planned. Because of its high acceleration, when wing failure occurs, it takes place within about a second from the time of launching. The few cases tested to date have shown fairly consistent results with duplicate firings and also in comparison with the low-acceleration bomb drop tests; however it is planned to test further for effects of acceleration.

Figure 4 is a photograph of the larger low-acceleration rocket (designated FR-1) shown with 45° sweptback test wings. Its weight is about 250 pounds, its acceleration from 2 to 4g and its top speed corresponds to a Mach number about 1.2. This rocket is equipped with a telemeter to transmit strain gage, breakwire, and acceleration records of the wings. A sample record (reference 5) will be shown subsequently.

Figure 5 shows a free-fall-bomb flutter vehicle. First successful telemetered flutter records were obtained with this type of vehicle. The bombs have been released at various altitudes up to 35,000 feet, and are accelerated by gravity to attain a Mach number from about 1.0 to 1.3. A sample record is given in another figure.

Figure 6 shows the first telemetered record obtained from a low-acceleration rocket test. This particular rocket carried two 45° sweptback wings as shown in figure 4. Flutter occurred at a Mach number of 0.67 in a symmetrical mode. In spite of large flutter amplitudes, however, one wing apparently did not break off. It may be of interest to mention that the ratio of flutter frequency to the wing torsional frequency was 0.55.

Figure 7 shows a telemetered record from a free-fall bomb vehicle carrying two 45° sweptback wings. (See reference 6.) Bending and torsion strain on one wing and torsion on the other are recorded. (Four channels were used in this case; it is expected to employ additional channels in some later tests.) This flutter occurred at $M = 0.92$, one wing failed at once, the other fluttered for another second or so subsequent to the first wing failure before it too failed. The flutter frequency was 0.38 that of wing torsion.

A composite plot is shown in figure 8 of some of the wind-tunnel, bomb, and rocket data for unswept uniform rectangular wings of various aspect ratios or rather semispan-chord ratios l/c. The abscissa is the Mach number and the ordinate is the ratio of flutter speed measured to flutter speed calculated on the basis of two-dimensional incompressible-flow considerations. The data shown are for wings of several different mass ratios, elastic axes, and center-of-gravity locations. The full curve represents theoretical (two-dimensional) calculations for mass ratio $\frac{m}{\rho c^2} = 50$ and center of gravity and elastic axes at 45 percent chord. The effect of Mach number and of variation of the semispan-chord ratio l/c is indicated by the data. For l/c from 3 to 6 there is only a small effect, while for $\frac{l}{c} = 1$ there is a fairly significant rise.

It will be recalled that extrapolations from theoretical considerations based on subsonic and supersonic linearized theory indicated that, for center-of-gravity locations forward of the midchord, the design critical range is the near sonic speed range. (It was also shown that the particular quantity $\frac{b\omega_\alpha}{c}$ (half chord times torsional frequency divided by sound speed) plays an interesting role as a basic nondimensional parameter, around which it appears that convenient empirical rules can be developed.)

In general the data of figure 8 indicate that the transonic range may be the determining factor in deciding the stiffness as far as wing flutter is concerned. Other data will be published in various NACA papers.

Figure 9 is a plot against Mach number of the effect on the flutter speed of rotating a uniform (4 inch × 4 inch) cantilever wing in the wind tunnel, the sweepback being changed by rotating the model mount. The problem of sweep brings into the flutter analysis several new problems which have thus far been only lightly touched upon by several workers. Thus, there is the problem of the modes of vibration, in particular for a curved or bent back elastic axis, involving a greater degree of coupling between bending and torsion, and there is the aerodynamic coupling in the finite-span problem.

It perhaps should be mentioned that for an infinite uniform yawed wing (yawed at an angle not near 90°) two-dimensional low-speed considerations indicate that the flutter speed increases as one over the cosine of the angle of sweep. However, the combined effects of the elastic and aerodynamic coupling, together with the finite-span problem, apparently result in no such favorable increase. In general it appears that up to 30° sweep there is only a very small increase in the flutter speed.

The rocket-data points (fig. 9) are for built-in 45° swept wings (of length 27 inches along the leading edge and chord 12 inches normal to the leading edge). The free-fall-bomb-data points are for a wing of dimensions 28 inches along the leading edge and 8 inches normal to leading edge. It may be seen that for 45° angle of sweep the wind-tunnel, rocket, and bomb data are in fair agreement.

Some effects have been found to be due to the manner in which the root was built in or the tip cut off; also models with large length to chord ratio tend to introduce higher mode effects leading to erratic sweep effects for low angles of sweep as in this figure.

Figure 10 shows some effects of sweep for models which had the same section parallel to the airstream (sheared back) and the same span normal to the airstream; that is the aspect ratio was kept constant. The lower curve gives the measured torsional frequency as a function of the sweep angle. Dimensional considerations indicate that this frequency should be constant (except for tip and root effects) for the sheared-back uniform wing and the data bear this out.

The flutter speed also appears to be relatively constant, though there is appreciable scatter. The data thus indicate that the flutter speed of a sweptback homogeneous wing (sheared back in the manner described) is about the same as the wing without sweep. The Mach number at flutter and the flutter frequency for the test points are also shown in the figure.

Figure 11 gives some results of an investigation on the effect of concentrated weights on the flutter of a cantilever wing. The investigation includes single and multiple weights, and the mass and its moments of inertia are varied, as well as the spanwise and cordwise positions in conjunction with uniform, tapered and swept-back wings. The figure is, however, for a uniform unswept cantilever $\left(\frac{l}{c} = 6\right)$ and for a single weight 93 percent of wing weight (reference 7). (The mass of the weight was constant for these tests but the polar moment of inertia about the elastic axis of the wing varied with the chordwise location.) The abscissa of the chart is the location of the weight along the span. The ordinate is the flutter speed measured with the weight on divided by the flutter speed without the weight (wing alone). Each curve is drawn for a single chordwise location of the weight; the center of gravity location of the weight is sketched in the figure.

It is noted that the rearward location of the weight lowered the flutter speed while the forward location raised the flutter speed. (There is a small decrease for the near inboard positions in all cases.) For the most forward chordwise location there was a range of span positions at which no flutter occurred below the divergence speed of the wing. However, with the weight at a tip location in this case a higher-frequency type flutter did occur. This effect probably depends on the zero airspeed frequency spectrum and hence is probably different as the aspect ratio of a given wing is changed.

The test data in this single chart corresponds to well over 100 flutter tests taken at Mach numbers around 0.3 to 0.4. A similar series of tests for the weight location near the wing

center of gravity has been run for Mach numbers up to 0.7 and showed the same trends as indicated in the figure.

Theoretical calculations for the flutter speed have been made for the case in which the chordwise location of the weight is near the elastic axis. The uncoupled modes were used in these calculations, and theory compared well with the experimental results. For weight locations far from the elastic axis, however, higher modes or coupled modes are probably required. An extension of the treatment of Goland and Luke (reference 8) for the work is being examined. Results of these calculations are not yet available.

The quantitative correlation of theory and experiment is the goal of this study. These data provide an opportunity for such a quantitative check and should prove useful in evaluating the degree of refinements necessary in both the elastic and aerodynamic parts of the theory in order to keep each in step with the other.

A selection of results obtained at the Langley Laboratory are presented here. Many things have been left unsaid and many more things have been left undone. Various recent aircraft company reports on aeroelastic problems exist to which specific reference here is not feasible. It is hoped that information may be obtained at high-speed conditions for the mixed subsonic-supersonic types of flow (for instance, on the effects of thick and thin sections, of rounded and sharp leading edges) to examine possible nonstationary effects of detached and attached strong shocks. Also measurements of aerodynamic derivatives in the near sonic and supersonic speed ranges require exacting experimental techniques and critical tests.

This talk has been only of potential flow or classical flutter. It is also desirable to examine the separated flow types of instability which particularly at high speeds may be due to a variety of causes. These instabilities may be associated with wide movements of the center of pressure and with regular breakaway and reattachment of the flow. In addition there is the interaction of the aerodynamic and elastic forces in the class of stability problems involving control effectiveness and control reversal. The whole field of aeroelasticity is pretty wide open and remains a challenging field of inquiry.

REFERENCES

1. Budiansky, Bernard, Kotanchik, Joseph N., and Chiarito, Patrick T.: A Torsional Stiffness Criterion for Preventing Flutter of Wings of Supersonic Missiles. NACA RM No. L7G02, 1947.

2. Garrick, I. E., and Rubinow, S. I.: Flutter and Oscillating Air-Force Calculations for an Airfoil in a Two-Dimensional Supersonic Flow. NACA TN No. 1158, 1946.

3. Garrick, I. E., and Rubinow, S. I.: Theoretical Study of Air Forces on an Oscillating or Steady Thin Wing in a Supersonic Main Stream. NACA TN No. 1383, 1947.

4. Barmby, J. G., and Teitelbaum, J. M.: Initial Flight Tests of the NACA FR-2, a High-Velocity Rocket-Propelled Vehicle for Transonic Flutter Research. NACA RM No. L7J20, 1947.

5. Angle, E. E.: Initial Flight Test of the NACA FR-1-A, a Low Acceleration Rocket-Propelled Vehicle for Transonic Flutter Research. NACA RM No. L7J08, 1947.

6. Clevenson, S. A., and Lauten, William T., Jr.: Flutter Investigation in the Transonic Range of Six Airfoils Attached to Three Freely Falling Bodies. NACA RM No. L7K17, 1947.

7. Runyan, Harry L., and Sewall, John L.: Experimental Investigation of the Effects of Concentrated Weights on Flutter Characteristics of a Straight Cantilever Wing. (Prospective NACA paper)

8. Goland, M., and Luke, Y. L.: The Flutter of a Uniform Wing with Tip Weights. Rep. No. 1-536-E-4, Midwest Res. Inst., Kansas City, Mo., Jan. 2, 1947.

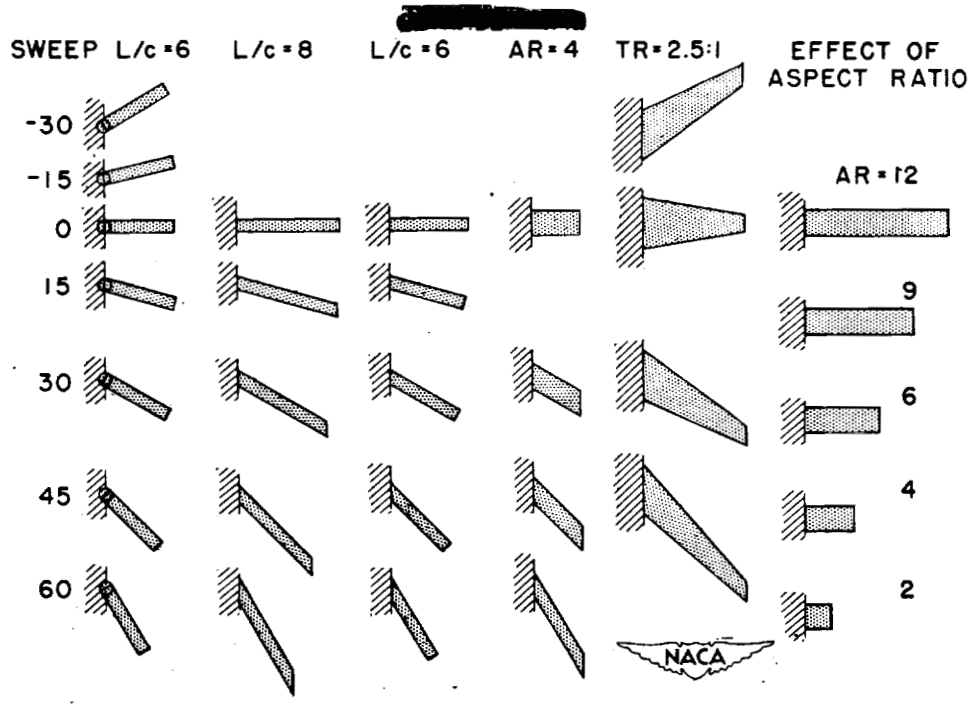

Figure 1.- Flutter-tunnel models.

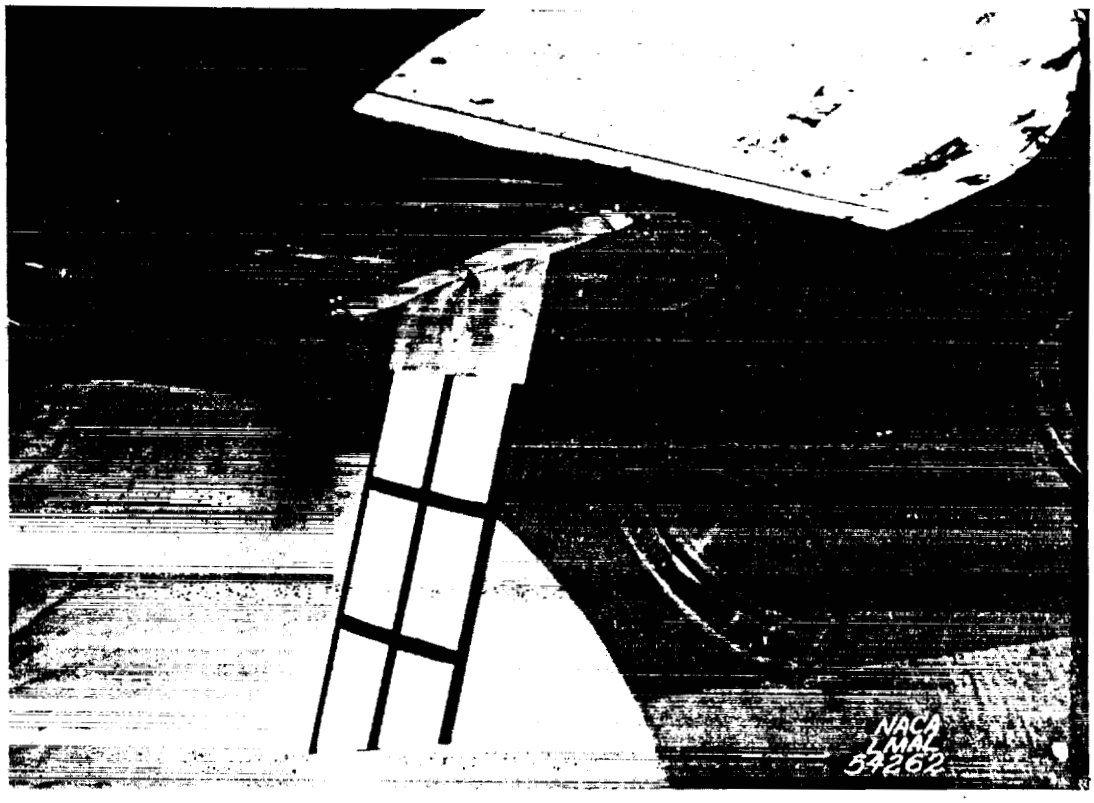

Figure 2.- Swept wing mounted as cantilever in flutter tunnel.

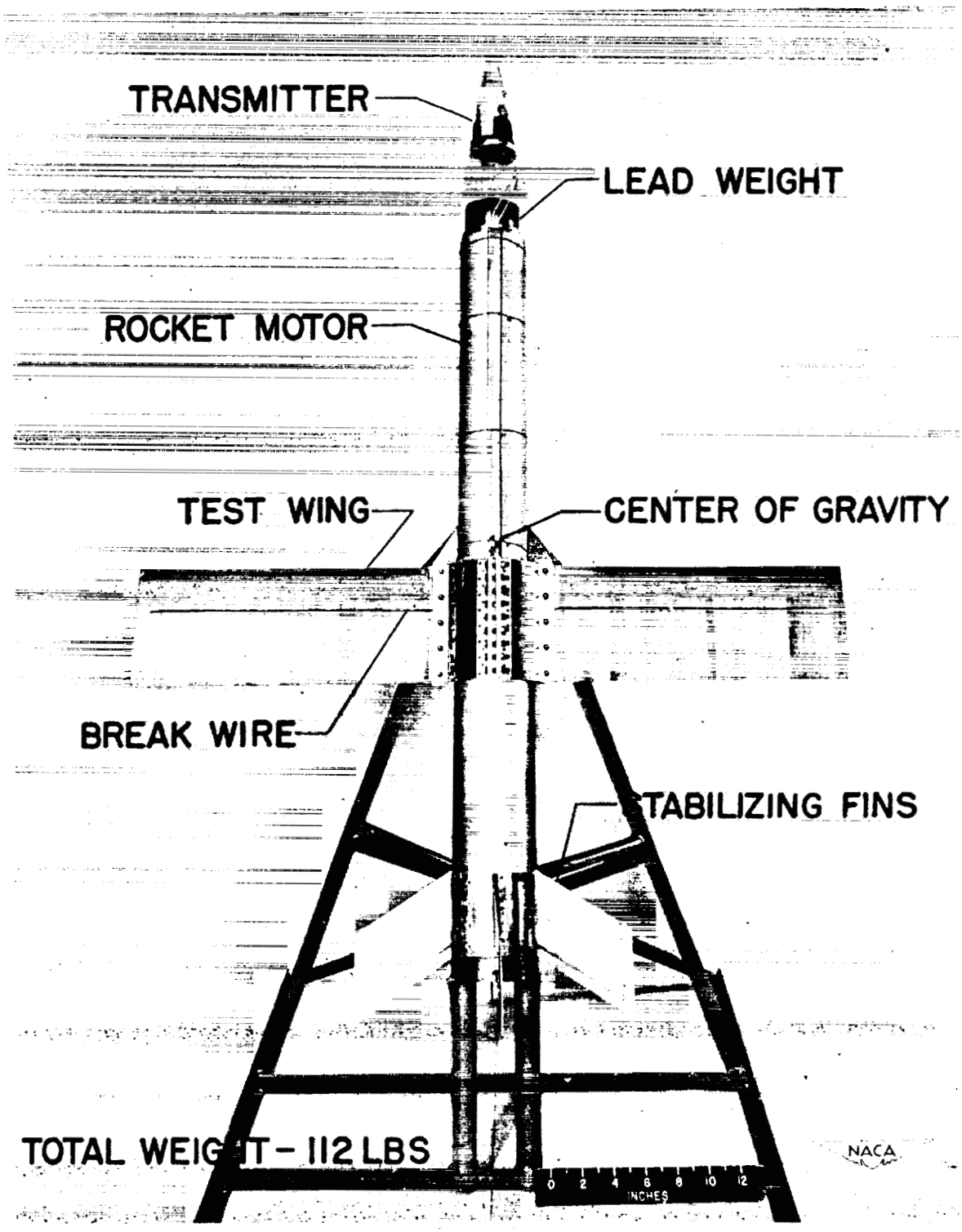

Figure 3.- High-speed-rocket flutter vehicle.

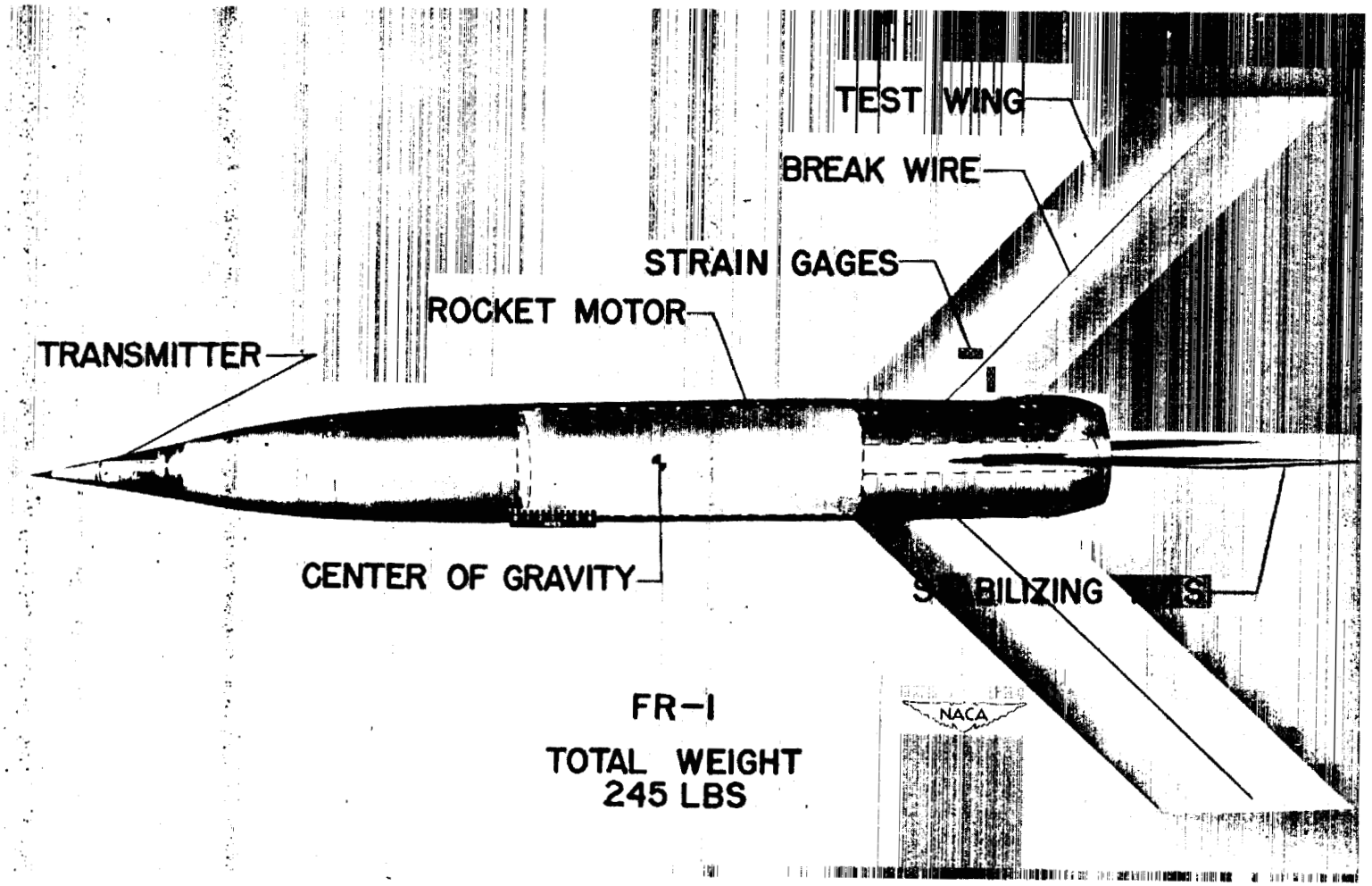

Figure 4.- Low-acceleration rocket (FR-1).

Garrick

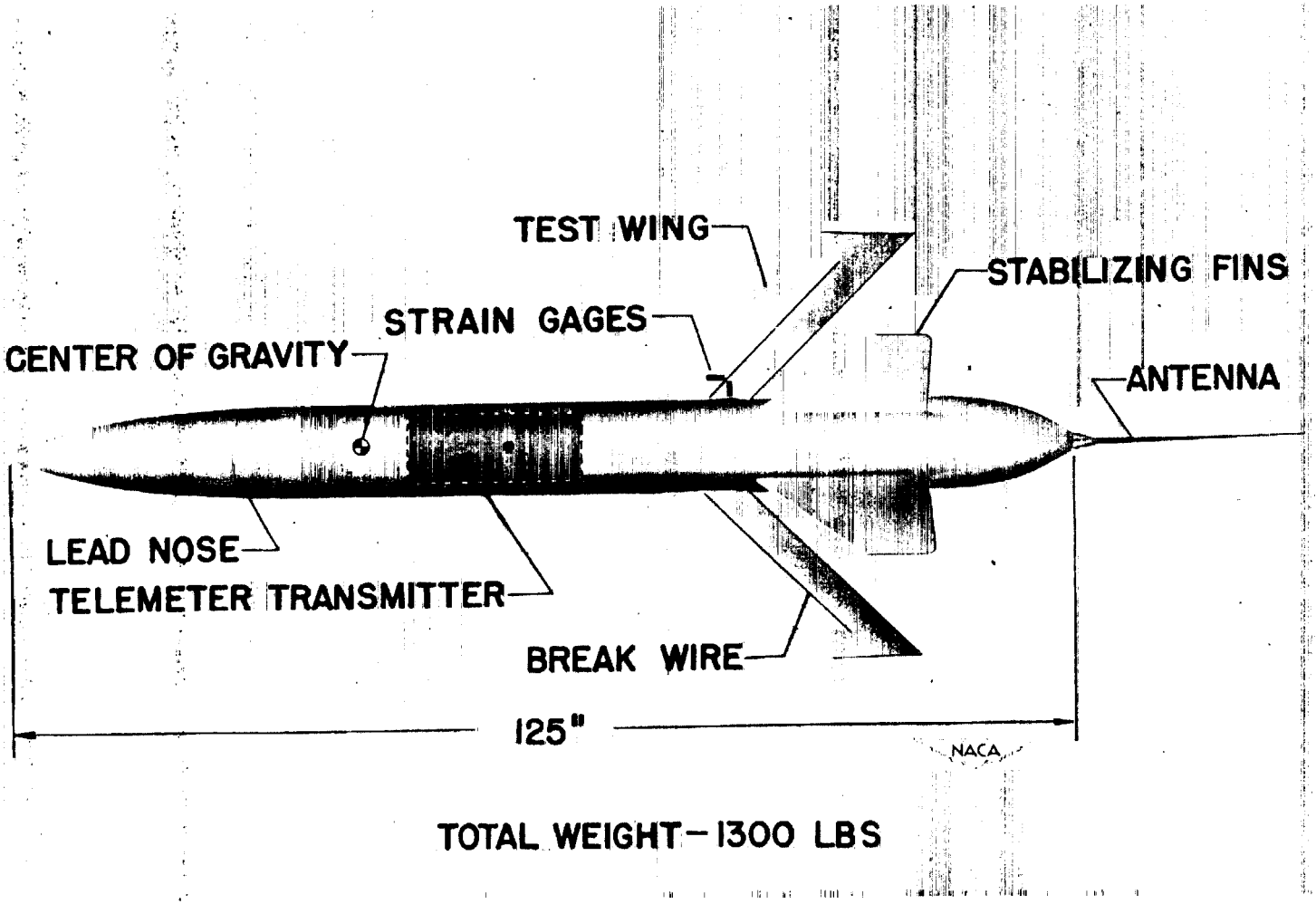

Figure 5.- Free-fall-bomb flutter vehicle.

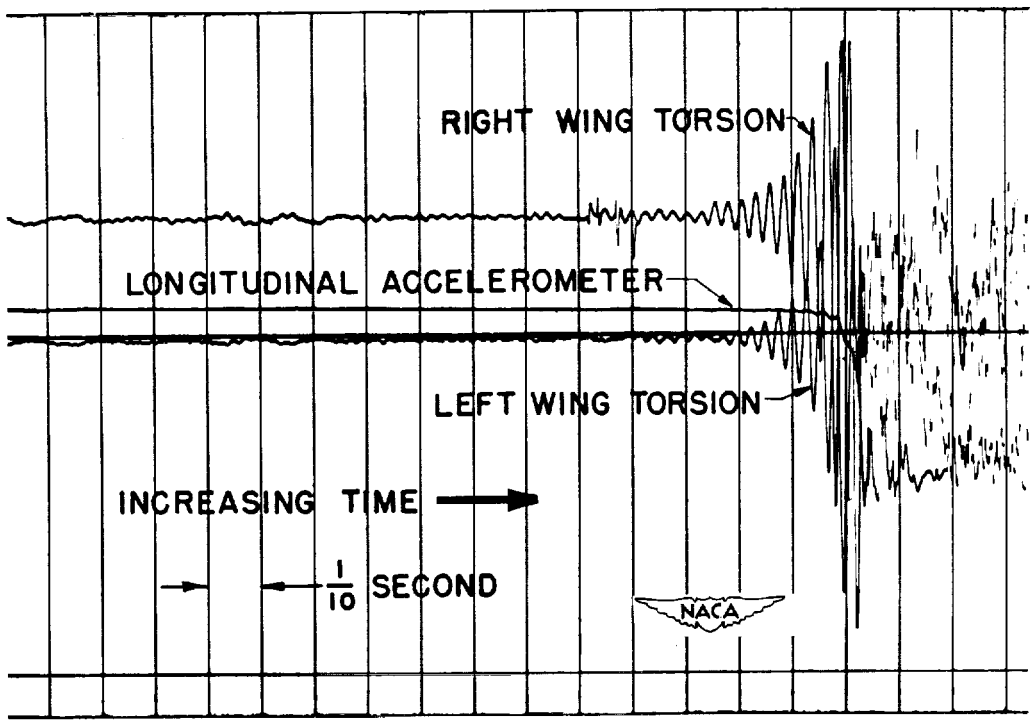

Figure 6.- Rocket telemeter record.

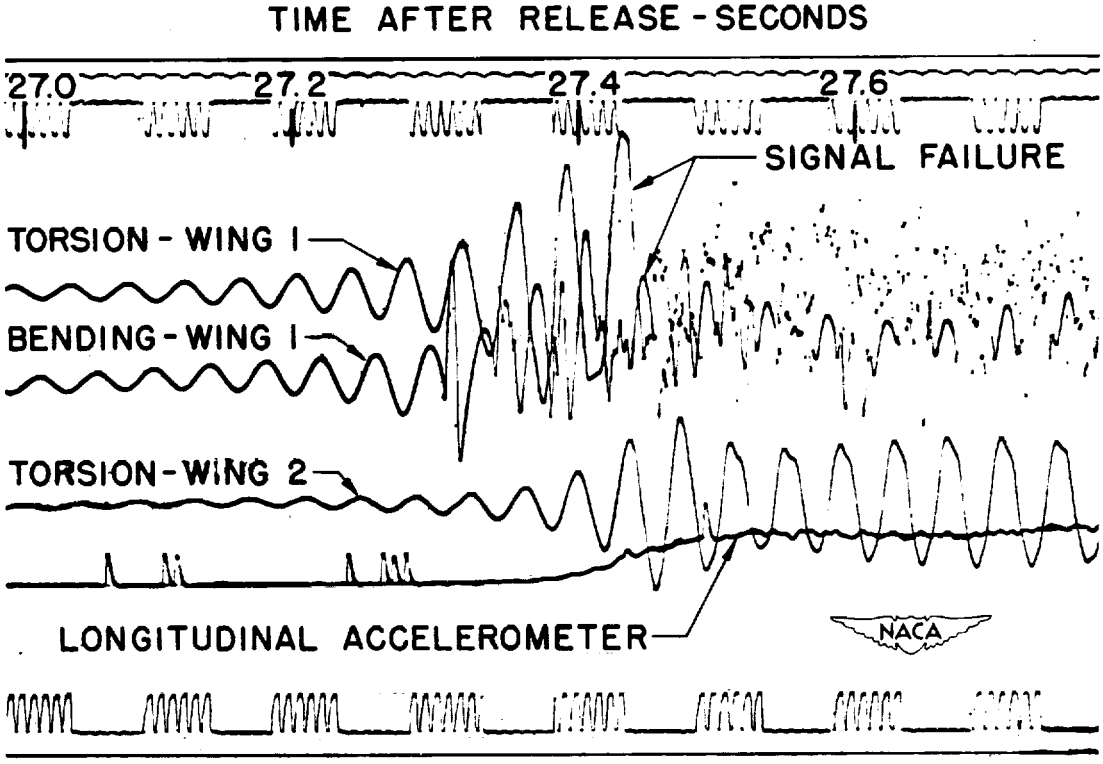

Figure 7.- Bomb telemeter record.

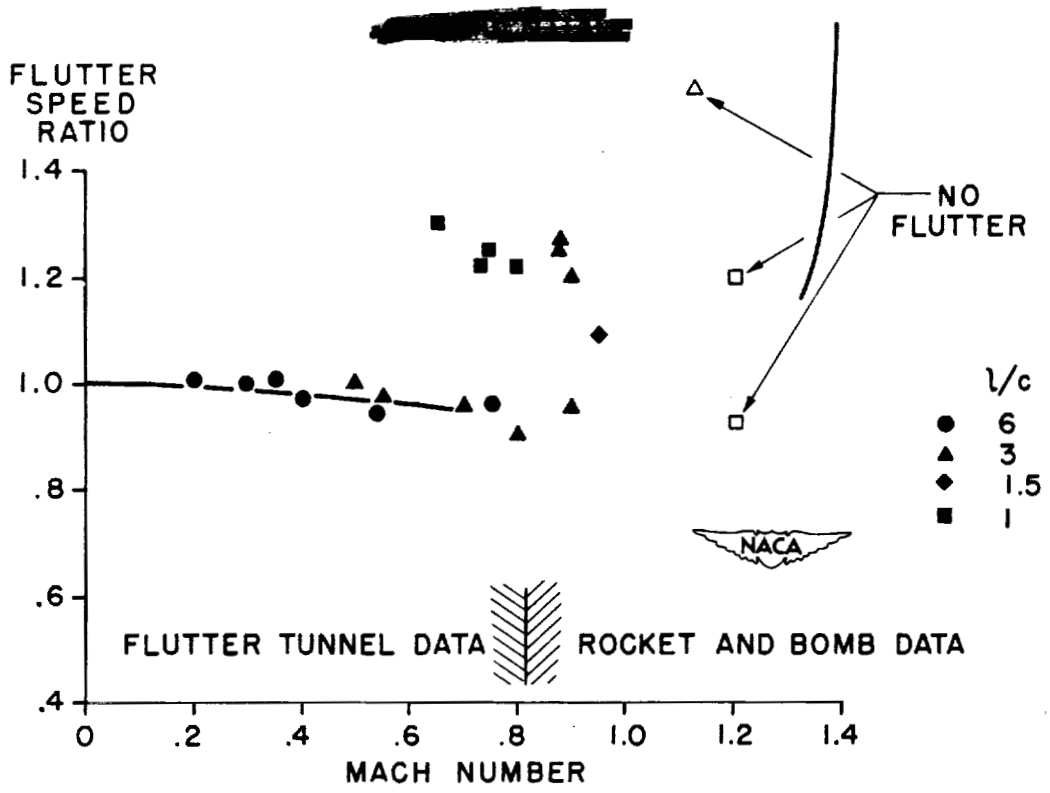

Figure 8.- Wing bending-torsion flutter.

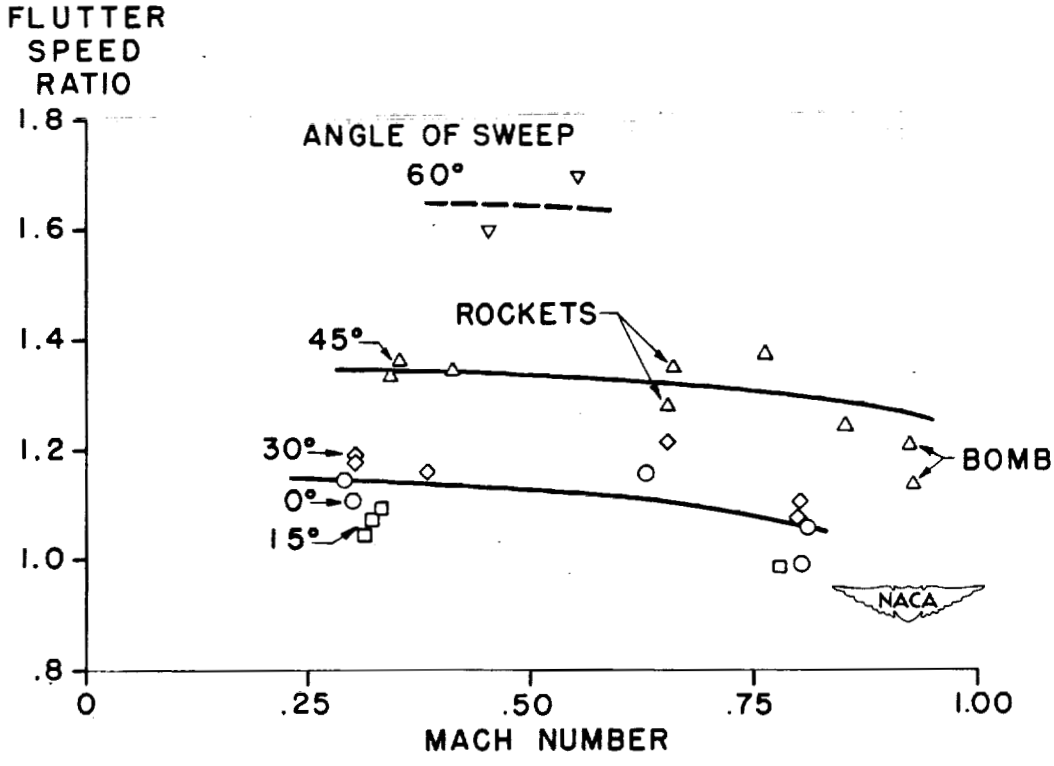

Figure 9.- Effect of sweep for rotated cantilever wing.

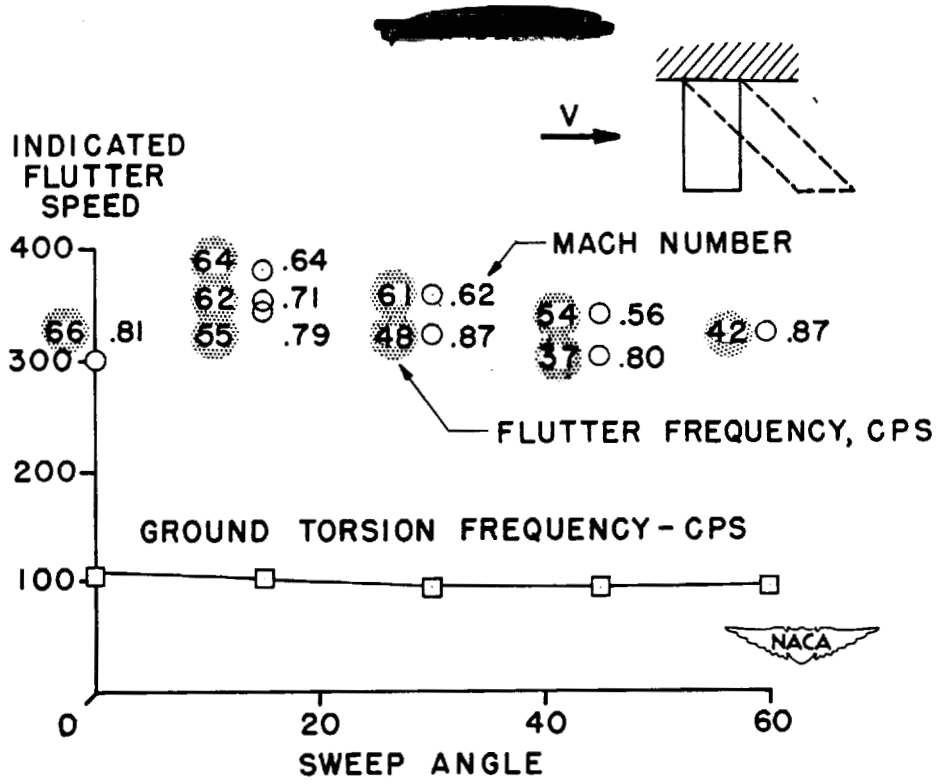

Figure 10.- Effect of sweep for sheared-back models.

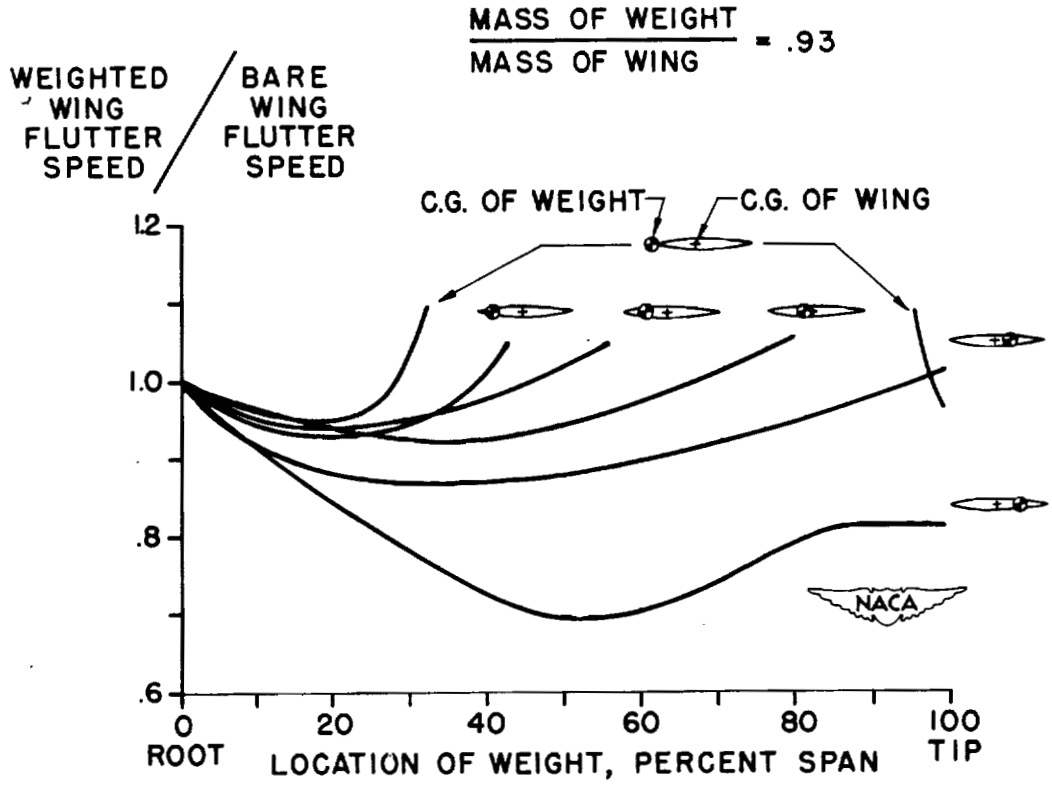

Figure 11.- Concentrated weights.